

Structural (B1 \rightarrow B8) Phase Transition in MnO under Pressure: Comparison of All-electron and Pseudopotential Approaches

Jindřich Kolorenč* and Lubos Mitás

Department of Physics, North Carolina State University, Raleigh, North Carolina 27695, USA

(Dated: December 20, 2018)

We employ the density functional theory to study a structural transition of MnO from B1 (rock-salt) to B8 (NiAs) structures that was observed experimentally at pressures around 100 GPa. We utilize all-electron description as well as norm-conserving pseudopotentials and demonstrate that these two approaches can significantly differ in quantitative predictions. We explicitly show that even small-core pseudopotentials exhibit transferability inaccuracies for quantities sensitive to the energy differences between high- and low-spin polarizations of valence electrons.

PACS numbers: 72.80.Ga, 71.15.-m, 71.20.-b, 64.30.+t

I. INTRODUCTION

Transition metal oxides have received a considerable attention of condensed matter physicists in the past several decades. One of the reasons for such an elevated interest is that the standard band theory methods, such as the density functional theory (DFT) represented by the local density approximation (LDA) or by its semi-local generalization (GGA), do not satisfactorily describe these materials. For example, the LDA/GGA predicts incorrect equilibrium crystal structure for FeO.^{1,2} In the case of equilibrium properties of MnO, these approximations perform reasonably well as was shown by several groups.^{3,4} The source of deficiencies of simple band theories is agreed to be underestimation of correlations among 3d electrons. Improved account for these correlations is needed to adequately capture Mott insulating mechanism and the competing charge transfer effects.

Several methods have been devised to resolve the issue of strongly correlated electrons, such as GW, LDA+U, self-interaction correction (SIC) or hybrid exchange-correlation functionals that combine local exchange from LDA or GGA with non-local Fock exchange. Performance of several of these approaches has recently been thoroughly compared in Ref. 5, using the pressure-induced high-spin to low-spin transition⁶ in MnO as a benchmark test. It turned out that although the current computational techniques work well for some aspect of the electronic structure (such as the equilibrium volume or the character of the ground state at ambient pressure), they are not quite dependable if one considers high-pressure properties of this material.

One of the goals of this paper is to provide additional benchmarks for the electronic structure of manganese oxide at high pressure, expanding thus the test set of Ref. 5. Our main message does not directly relate to the 3d electrons but to a rather surprising finding that the deep core states and the type of method used for their description can significantly influence certain properties generally considered to be related to the valence electrons only. An example of such a quantity is the critical pressure P_c for the pressure-induced transition from B1

(rocksalt) to B8 (NiAs) structure that has been reported recently.^{7,8} This transition is accompanied by a collapse of the local magnetic moments of Mn atoms⁸ as well as with electronic transition to a metallic state.⁹

Another key motivation for this study of core-valence interactions in crystalline MnO is our interest in applications of quantum Monte Carlo (QMC) techniques to transition metal oxides and other materials containing strongly correlated electrons. The accurate representation of physical ions by norm-conserving pseudopotentials is essential for obtaining meaningful and predictive quantum Monte Carlo results and it is therefore crucial to assess the accuracy and limits of such pseudopotential Hamiltonians. Ideally, one would compare results of pseudopotential QMC with all-electron QMC. Unfortunately, such a route is prohibitively computationally expensive at present. We have therefore decided to carry out a careful study within the DFT, Hartree-Fock (HF) approximation and combination of these methods, since the accuracy of one-particle orbitals is important in QMC as mentioned below and explained elsewhere.^{10,11} Similar problems were investigated in several density-functional studies (e.g., Refs. 12,13,14,15) and provided important signals that the choice of the methods and treatment of pseudopotentials can affect the final results.

Our study provides new insights in several important and complementary directions. First, we employ Dirac-Fock pseudopotentials, which nominally should not require any additional corrections (such as the DFT non-linear core correction as commented later on). The reason for this choice is that these pseudopotentials were designed to be accurate for correlated wave function calculations and, in fact, several tests have been carried out within both post-Hartree-Fock (configuration interaction) and quantum Monte Carlo methods with quite satisfactory results.^{10,11} Second, we wanted to quantify the pseudopotential vs. all-electron differences within the DFT, HF and hybrid functionals since our previous¹⁰ (and current preliminary) calculations show that the hybrid functionals provide the most optimal one-particle orbitals, which minimize the fixed-node error in the quantum Monte Carlo method. The use of two independent codes and basis sets provides a solid computational

framework for accurate benchmarking of these issues. In addition, study of high-pressure phase adds another important test, since the dramatic changes in electronic structure probe the pseudopotentials in the regime, for which their reliability cannot be taken for granted.

II. AMBIENT PRESSURE

Before we proceed with investigation of the B1 \rightarrow B8 phase transition we first concentrate on energy differences between various magnetic phases at ambient pressure. We apply the all-electron method side by side with the pseudopotential approach. For this purpose we have modified the WIEN2k package¹⁶ so that one can use either the original all-electron core solver or the norm-conserving pseudopotentials (PP). The valence states are expanded in the LAPW basis (extended by local orbitals) in both cases. This allows for a systematic comparison of full cores with PPs, since the only point where such calculations differ is the treatment of the core electrons. Similar combination of LAPW and pseudopotentials was already used to look into some aspects of PP applications to transition metals.¹³

In order to minimize errors associated with partitioning core-valence correlations in pseudopotential calculations, we have chosen pseudopotentials with $3s$ and $3p$ states in the valence space, so that the eliminated core corresponded to the Ne atom. We tested two types of norm-conserving PPs constructed from Dirac-Fock atomic solutions. The first one, denoted as YN, is a soft pseudopotential generated using Troullier-Martins construction.¹⁷ The second PP, labeled as STU, is the so-called energy-adjusted pseudopotential,¹⁸ which has the $-Z_{eff}/r$ attractive ionic part retained.

In addition to performance of pseudopotentials we were interested in the impact of exact exchange on electronic structure of manganese oxide. To this end we have employed the CRYSTAL2003 code¹⁹ that uses Gaussian type atomic orbitals as a basis for one-particle wave functions. In the following we refer to this method as LCAO. The exact exchange was studied by means of two hybrid exchange-correlation functionals. We utilized B3LYP as well as somewhat simpler PBE0 functional. The later one is schematically written as

$$E_{xc}^{PBE0} = aE_x^{HF} + (1-a)E_x^{PBE} + E_c^{PBE}, \quad (1)$$

where E_x^{PBE} and E_c^{PBE} are exchange and correlation parts of the PBE-GGA,²⁰ E_x^{HF} is the exact (Fock) exchange and $a > 0$. This type of hybrid mixing has the advantage that it directly relates to the PBE-GGA approximation employed in our LAPW calculations. We use a rather small value $a = 1/10$ for the Fock mixing weight to account for the (nearly) metallic behavior at pressures we are going to investigate later. In the rest of the paper we abbreviate this functional as PBE0₁₀. With the standard choice of $a = 1/4$ (Ref. 21) we ran into serious difficulties in converging the Kohn-Sham equations

XC functional	core	Δ (eV)	$\Delta^{all} - \Delta^{PP}$ (eV)	m (μ_B)
GGA, LAPW	all-electron	-2.29		4.23
	YN	-2.80	0.50	4.29
	STU	-2.94	0.65	4.32
GGA, LAPW, non-relativistic	all-electron	-2.31		4.23
	YN	-2.78	0.47	4.29
	STU	-2.92	0.61	4.31
GGA, LCAO	all-electron	-2.39		4.59
	YN	-2.83	0.44	4.63
	STU	-2.96	0.57	4.64
PBE0 ₁₀ , LCAO	all-electron	-3.50		4.70
	YN	-3.82	0.33	4.71
	STU	-3.91	0.41	4.71
B3LYP, LCAO	all-electron	-4.15		4.74
	YN	-4.24	0.09	4.74
	STU	-4.33	0.18	4.74
HF, LCAO	all-electron	-12.73		4.93
	YN	-12.55	-0.18	4.91
	STU	-12.18	-0.55	4.90

TABLE I: Energy difference $\Delta = E_{AFM} - E_{NM}$ per MnO at lattice constant 4.43 Å together with local moments m formed on Mn atoms in the AFM phase. The disagreement between Δ^{all} and Δ^{PP} has opposite signs in PBE-GGA and Hartree-Fock (HF) calculations and is considerably reduced for hybrid functionals, especially for B3LYP.

when the lattice was compressed to the extent needed to reach the B1 \rightarrow B8 transition. Another alternative and possibly more sophisticated way around this problem is to employ a screened exchange instead of the full one.^{5,22}

The outcome of the electronic structure methods introduced above is summarized in Tab. I where we compare two electronic phases of MnO in the rocksalt structure at equilibrium lattice constant: the nonmagnetic (NM) state and the state with antiferromagnetic (AFM) ordering of adjacent Mn (111)-planes, i.e., the so-called type-II antiferromagnet. The AFM phase represents the ambient pressure ground state. In the case of the LAPW method, the basis size and the density of k -point mesh was converged down to 1 or 2 mRy (~ 0.03 eV) in obtained total energies per formula unit. The Gaussian basis set for the LCAO methods was chosen large enough to reproduce the (nonrelativistic) LAPW/GGA results (see Tab. I).

Since we utilized only small-core pseudopotentials we expected only minor discrepancies between the all-electron and PP calculations. However, this assumption turned out not to be entirely correct. The results listed in Tab. I show that both *explicit presence of the core* and *the method which is employed* do matter. The difference between the all-electron and pseudopotential techniques varies from +0.6 eV/MnO within the PBE-GGA functional to -0.6 eV/MnO in the Hartree-Fock method combined with the STU PP. While contributions of this

magnitude might not be always relevant, for the purpose of comparing energies of different magnetic phases or in high pressure transitions such a difference turns out to be very significant.

In addition to the antiferromagnetic and nonmagnetic B1 phases we included into our investigation also the ferromagnetically (FM) ordered B1 structure. This time the energy difference $\Delta = E_{AFM} - E_{FM}$ stays virtually the same irrespective of the the core treatment used. This indicates that the sensitivity of Δ to the description of the core electrons is related to difference in magnetic moments of the two involved states — the local moments in FM and AFM phases are almost identical, approximately $4.5 \mu_B$ (see Tab. I), whereas they are by definition zero in the NM state. More detailed evidence pointing in this direction is presented within the high pressure study below.

Several comparisons of all-electron and small-core pseudopotential data can be found in the literature in connection with the so-called non-linear core correction (NLCC).¹² LDA studies of $3d$ atoms²³ and transition metal bearing diatomic molecules²⁴ show that without the NLCC the errors in energetics, associated with small-core pseudopotentials, are generally of the order of tenths of eV, which is in agreement with our observations made in solids. The non-linear core correction is demonstrated to be capable of removing a large portion of these errors.^{23,24}

We have decided not to include the NLCC in our study for the following reason. The NLCC concept, correcting for linearization of core-valence correlations inherent to the standard norm-conserving pseudopotential technique, is not systematically transferable to methods using exact exchange, i.e., to hybrid exchange-correlation functionals, or to many-body methods such as quantum Monte Carlo. For these approaches it is therefore important to assess how accurately the actual pseudopotential Hamiltonian represents the physical ion. Indeed, our study is a test whether this appears to be true for a variety of magnetic states, range of pressures and different methods. In the next section we provide additional benchmarks for MnO molecule and Mn atom, which clearly delineate the consistency of the used PPs and also suggest what is the reason for the discrepancies we found. Although the discussion of pseudopotential constructions is out of the scope of this paper we just note that the core-valence partitioning is more straightforward within the Dirac-Fock approximation than within the DFT due to the rather complicated nonlinear dependence of the DFT exchange-correlation functional on the density. In fact, one set of the Dirac-Fock pseudopotentials we employed has been used in high-accuracy correlated calculations by quantum-chemical methods in a routine manner without additional corrections and with satisfactory results for equilibrium properties of molecular systems.^{10,11,25}

method	core	D_e (eV)	$D_e^{all} - D_e^{PP}$ (eV)
ROHF	all-electron	-0.86	
	YN	-0.85	-0.01
	STU	-0.94	0.08
UHF	all-electron	0.69	
	YN	0.66	0.03
	STU	0.60	0.09

TABLE II: Dissociation energy D_e of MnO molecule at a bond length 1.64 Å calculated with restricted open shell (ROHF) and unrestricted (UHF) Hartree-Fock methods. Both the molecule and Mn atom are in a high-spin configuration with spin multiplicity 6.

method	core	Δ (eV)	$\Delta^{all} - \Delta^{PP}$ (eV)
E_{ls} with ROHF E_{hs} with ROHF	all-electron	6.59	
	YN	6.69	-0.10
	STU	6.76	-0.17
E_{ls} with ROHF E_{hs} with UHF	all-electron	8.42	
	YN	8.50	-0.08
	STU	8.61	-0.19

TABLE III: Energy difference $\Delta = E_{ls} - E_{hs}$ between high-spin ($\sigma^1 \delta^1 \bar{\delta}^1 \pi^1 \bar{\pi}^1$, multiplicity 6) and low-spin ($\sigma^1 \delta^2 \bar{\delta}^2$, multiplicity 2) configurations of MnO molecule calculated with Hartree-Fock methods. Bond length is 1.64 Å as in Tab. II.

III. TESTING THE PSEUDOPOTENTIALS IN Mn ATOM AND MnO MOLECULE

The results presented in the preceding paragraph might appear somewhat surprising, since very small errors generated by small-core PPs have been observed in isolated atoms.^{10,18} In particular, our Hartree-Fock tests of atomic $s \rightarrow d$ transfer energies, i.e., differences between high-spin and low-spin states in the isolated atom (not explicitly shown), turned out the same no matter whether all-electron or pseudopotential Hamiltonian has been employed. In addition, our previous calculations within high-accuracy quantum Monte Carlo reproduced the experimental $s \rightarrow d$ transfer energy within 0.1 eV.¹⁰ This suggests that the norm-conserving Dirac-Fock construction provides accurate PP Hamiltonian, which represents the physical ion within both the mean-field and correlated many-body methods with accuracy better than 0.1 eV. A question then arises where is the origin of the discrepancies reported in the previous section. Is it something related solely to the solid state environment or can it be detected as soon as chemical bonds are formed? The LDA study of molecules containing transition metal atoms, Ref. 24, suggests that the second statement is indeed true. To verify this we performed several Hartree-Fock calculations to demonstrate that such a conclusion

is not only LDA specific.

Tables II and III show results obtained using the GAMESS code²⁶ with large uncontracted basis sets for pseudoatoms and with natural atomic orbitals^{27,28} for all-electron atoms. Whenever only same spin states are involved, as is the case of the dissociation energy D_e (Tab. II) of the ground state of MnO molecule, the all-electron and pseudopotential results agree quite well. Especially when YN pseudopotential is used, the difference $D_e^{all} - D_e^{PP}$ falls quite clearly below resolution of the basis sets employed. In addition, tests done with highly correlated multi-determinant Slater-Jastrow trial wave functions and with fixed-node diffusion Monte Carlo reproduced the experimental binding energy within 0.1 eV.¹¹ Therefore, even cohesive properties of the PP Hamiltonian look correct both within mean-field and many-body correlated methods.

A small but visible inconsistency between all-electron and pseudopotential approaches suddenly appears if one considers a *high-spin to low-spin transition in the molecule* (Tab. III). Electronic configurations are $\sigma^1\delta^1\bar{\delta}^1\pi^1\bar{\pi}^1$ for the high-spin and $\sigma^1\delta^2\bar{\delta}^2$ for the low-spin state. Comparison of quantities $\Delta^{all} - \Delta^{PP}$ between Tabs. I and III shows that the discrepancies in the solid are almost three times larger than in the molecule. This is understandable since the Mn bonding in solid is enhanced by the octahedral arrangement of the oxygen atoms. Trying to estimate how much stronger this effect would be from the size of cohesions one finds that the ratio of (experimental) binding energies^{29,30} of the two systems is 9.5 eV/3.8 eV = 2.5. The key question which therefore remains to be answered is: where is this effect coming from? We believe that the bonding environment is the key consideration for resolving this issue. In an isolated atom the d electrons have freedom to expand away from the nucleus and indeed one finds that the atomic d orbitals for low-spin states are very diffuse. In the presence of chemical bond, say, in a molecule, such an expansion is not favorable, since bonding tends to localize the states even for doubly occupied d channels. In a solid this is even more pronounced as the Mn atom is encapsulated in the octahedron of oxygens. This enhances the amount of charge in the d states inside the core. The cause for the spin related discrepancies then becomes apparent — it is the bonding (or chemical) “pressure”.

IV. SOLID AT HIGH PRESSURES (GGA)

In order to examine the high pressure behavior of MnO, namely the B1 \rightarrow B8 transition, we have carried out a series of LAPW/GGA calculations⁴¹ for the type-II antiferromagnetic phase in the B1 structure and for the B8 structure with ferromagnetic as well as antiferromagnetic ordering of hexagonal Mn planes.⁴² The critical pressure P_c and volume change at the B1 \rightarrow B8 transition are listed on the first two lines of Tab. IV. The arrangement of local moments is found to change from AFM to

method	P_c (GPa)	V_{B1} (Å ³)	V_{B8} (Å ³)	m_{B1} (μ _B)	m_{B8} (μ _B)
GGA, all-el. LAPW	43	18.15	15.76	3.8	2.3
GGA, YN LAPW	67	17.01	14.98	3.9	2.4
PBE0 ₁₀ , all-el. LCAO	117	15.48	13.71	4.4	2.0
PBE0 ₁₀ , YN LCAO	125	15.12	13.17	4.4	2.0

TABLE IV: Critical pressures for the B1 AFM \rightarrow B8 FM phase transition as calculated with various methods. Also indicated are volumes (per formula unit) and the local magnetic moments on Mn atoms for both phases at the transition.

FM across the transition. The choice of the magnetic ordering in the high pressure phase is not well resolved, however, since the energy difference between B8 AFM and B8 FM phases at the relevant volumes is comparable to our 2 mRy precision estimate. The Fermi level lies in the gap between bands of the Kohn-Sham eigenvalues from ambient pressure all the way up to the transition in the case of the B1 AFM phase, whereas it is located inside a band for both studied B8 phases above and also well below P_c . These qualitative features do not change if full cores or pseudopotentials are used. The variation in quantitative aspects is, on the other hand, quite sizeable. For instance, the difference in the transition pressure P_c is as large as 25 GPa.

The GGA predictions are rather far from experimental P_c around 100 GPa^{7,8,9} and from a non-magnetic high pressure phase⁸ observed at room temperature (our calculations would support a paramagnetic phase at this temperature, at best). This is not surprising as the GGA is not expected to approximate the electronic structure of MnO very accurately. At the same time, the pressure $P_c = 67$ GPa resulting from our PP calculations is in a good agreement with results of Fang *et al.*³¹ who obtained $P_c \approx 60$ GPa with a plane-wave pseudopotential approach. The remaining few GPa might originate in the full structure optimization performed in Ref. 31. For the sake of simplicity, we have neglected the rhombohedral distortion in the B1 AFM phase and have not optimized the c/a ratio in the B8 phases. Instead we used a constant value $c/a = 2.0$ consistent with outcome of Ref. 31 and slightly smaller than $c/a \approx 2.1$ suggested by x-ray spectroscopy.⁸

Figures 1 and 2 relate the discrepancy between the two distinct core electron treatments to magnetic moments formed on manganese atoms. The quantity we use to measure the difference between all-electron and pseudopotential total energies is defined as

$$\varepsilon(V) = E^{all}(V) - E^{PP}(V) - [E^{all}(V_0) - E^{PP}(V_0)], \quad (2)$$

where V_0 stands for a reference volume. We use $V_0 = 21.7 \text{ Å}^3$ per formula unit in the B1 phase (Fig. 1) and $V_0 = 23.4 \text{ Å}^3$ per formula unit in the B8 phase (Fig. 2). In the rocksalt structure, the difference ε remains almost constant as long as the spin polarization does not change,

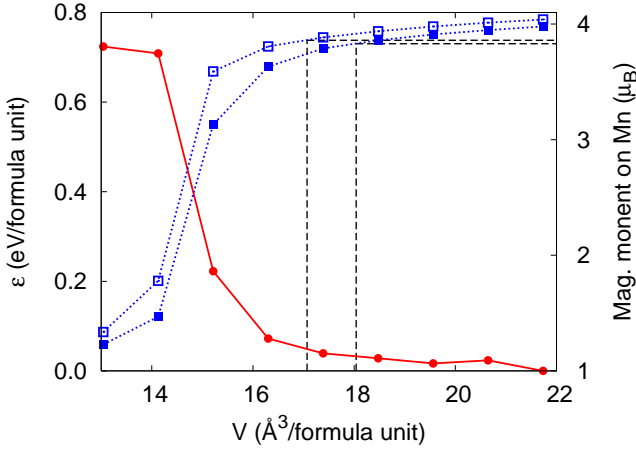


FIG. 1: (color online) Difference between all-electron and pseudopotential total energies, Eq. (2), as calculated for the B1 AFM structure within LAPW/GGA method (bullets). Also shown is magnetic moment on the Mn atom with all-electron core (full squares) and YN pseudopotential (empty squares). The slight enhancement of local moments when pseudopotentials are introduced, visible also in Tabs. I and IV, is consistent with other reports.^{13,32} Volumes at the transition to the B8 FM phase are indicated as well.

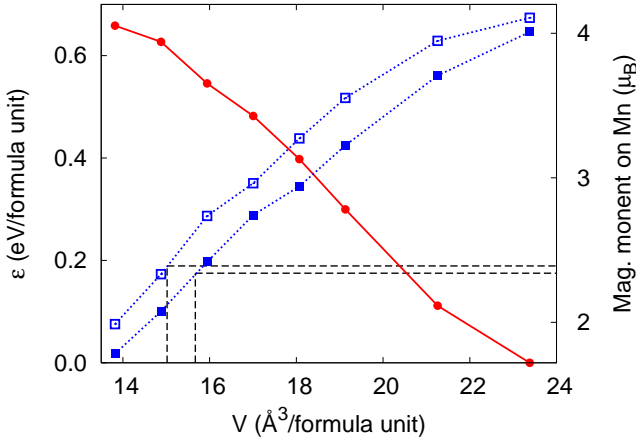


FIG. 2: (color online) Same quantities as in Fig. 1 but for B8 FM structure.

and jumps up at the high-spin to low-spin transition.⁶ The main reason for the 25 GPa inconsistency in the critical pressure P_c lies in the B8 phase, however, since rather high pressure is necessary for the high-spin to low-spin transition in the rocksalt structure. In the B8 phase the magnetic moment decreases gradually with volume compression and this reduction is accompanied with a gradual change of the difference ε that reaches an appreciable value at the point of the phase transition (see Fig. 2). The fact that the variation of the total energy difference ε apparently follows the evolution of spin polarization suggests that some type of spin-dependent pseudopotentials, possibly those introduced in Ref. 33, might bring the all-electron and pseudopotential results closer

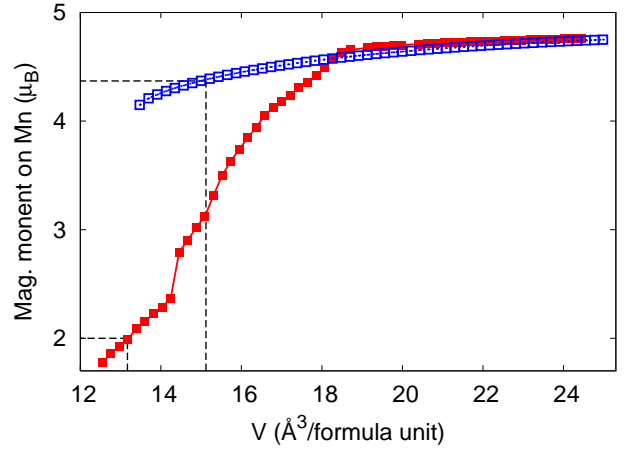


FIG. 3: (color online) Magnetic moment on Mn atom in B1 AFM (empty squares) and B8 FM (full squares) phases as calculated using the PBE0₁₀ functional. Values are taken from YN PP calculation, corresponding all-electron data are virtually indistinguishable. Transition volumes are shown as well.

together.

V. SOLID AT HIGH PRESSURES (HYBRID FUNCTIONAL)

To evaluate how the exact exchange influences the critical pressure of the B1 \rightarrow B8 transition we repeated the calculations with the PBE0₁₀ functional as shown on the last two lines of Table IV. We can see that already a small admixture of exact exchange moves the critical pressure P_c way above the GGA prediction, just a little higher than experimentally observed. Corresponding volumes of the phases above and below the transition are also very close to the experimental results.⁸ We would like to emphasize, however, that this study is targeted on methodology rather than on precise comparison with experiments since the latter goal would certainly require detailed geometry optimizations. The overall picture of the transition within PBE0₁₀ stays the same as with the GGA, the rocksalt phase is an insulator, the B8 phase is a metal. The magnetic moments collapse from $4.4 \mu_B$ to $2.0 \mu_B$ as the MnO is compressed across the transition. (Note that there are slight inconsistencies in comparisons of LAPW and LCAO local magnetic moments due to their different definitions.) The evolution of the magnetic moments with decreasing volume is shown in Fig. 3. The tendency of the Fock exchange towards electron localization is clearly visible, the decrease in moments is delayed to a lower volume in both B1 and B8 phases as compared to the GGA results displayed in Figs. 1 and 2. In the rocksalt structure we actually see no high-spin to low-spin transition in the interval of examined volumes.

The discrepancy between all-electron and pseudopotential approaches is greatly reduced when a hybrid func-

tional is used. Following the discussion of the GGA results one might expect that this reduction is accompanied by limited spin changes. However, the Fig. 3 demonstrates that this not the case and therefore we conclude that the core treated by PBE0₁₀ is more inert and is less sensitive to changes of the local moment formed by valence electrons.

VI. CONCLUSIONS

Our findings complement several other reports found in the literature indicating that application of pseudopotential based techniques to transition metals and their compounds is a delicate task.¹⁴ In particular, we can mention discrepancies in magnetic properties of the vanadium surface^{34,35,36} or inconsistencies in predictions of the ground state of Ce₂O₃^{37,38} found between pseudopotential and all-electron methods. In these studies, however, the large-core (Ar) PPs were utilized. The difficulties with pseudopotentials are then attributed to the semi-core 3s and 3p states that have too large overlap with the valence 4s and 3d electrons to be accurately represented by a “rigid core”. In the same time, the semi-core states are usually too localized to be efficiently included in the valence space.⁴³ This type of argument, however, cannot explain the variations in the B1 → B8 transition pressure presented in this paper, since we treat the 3s and 3p states as valence degrees of freedom. Our observations suggest that one should carefully examine transferability of pseudopotentials between different spin states even in the case of small-core PPs, especially if the phenomena under investigation involve variations in local magnetic moments.

Overall implications of our results are rather straightforward to explain. The 3d states have no counterparts of the same symmetry in the core and therefore an appreciable amount of the d charge density is localized in the core region. Consequently, changes in the local moments can influence the core states and vice versa. As we have verified, this is not detectable in isolated atoms, where the

all-electron and pseudopotential results agree very well, nor in equilibrium ground state cohesion energies, which do not involve dramatic changes in the local moment on the Mn atom. This is true not only for the mean-field methods employed in this study, but also for highly accurate quantum Monte Carlo tests done previously.^{10,11} These results suggest that the PP Hamiltonian is consistent and accurate. The discrepancy appears and becomes visible when the *high-spin/low-spin differences* become involved in bonds. The localization of the d states due to the chemical environment pushes larger fraction of the charge into the core and inaccuracies of various methods become more pronounced. The direction of the biases, which we found, is also not very difficult to understand. The LDA and GGA functionals are well-known to incline towards more smooth and homogeneous densities with exaggerated softening of electron-electron repulsion. On the opposite side is the Hartree-Fock method, which tends to localize the states since that enhances the exchange contributions (the only mechanism, through which HF can decrease the energy). The key point is that these biases affect *all degrees of freedom* of the given system, including, in all-electron calculations, also the core states. Therefore, the cores are “softened” in the LDA/GGA approaches and “tightened” in the HF approximation. In the PP case the core is rigid and therefore the bias from core states is absent that leads to seemingly better (closer to experiment) results for the transition pressures. Finally, these results could be of interest not only for high-pressure solids but also for other transition metal systems with significant magnetic moment changes such as biomolecular reaction centers or catalysis.

Acknowledgments

We acknowledge support by NSF DMR-0121361 and EAR-0530110 grants and we would like to thank for the kind consent to modify the WIEN2k code by P. Blaha.

* On leave from Institute of Physics, Academy of Sciences of the Czech Republic, Na Slovance 2, CZ-18221 Praha 8, Czech Republic

¹ I. I. Mazin, Y. Fei, R. Dawns, and R. Cohen, *American Mineralogist* **83**, 451 (1998).

² Z. Fang, K. Terakura, H. Sawada, T. Miyazaki, and I. Solovyev, *Phys. Rev. Lett.* **81**, 1027 (1998).

³ J. E. Pask, D. J. Singh, I. I. Mazin, C. S. Hellberg, and J. Kortus, *Phys. Rev. B* **64**, 024403 (2001).

⁴ K. Terakura, T. Oguchi, A. R. Williams, and J. Kübler, *Phys. Rev. B* **30**, 4734 (1984).

⁵ D. Kasinathan, J. Kuneš, K. Koepernik, C. V. Diaconu, R. L. Martin, I. Prodan, G. E. Scuseria, N. Spaldin, L. Petit, T. C. Schulthess, and W. E. Pickett, *cond-*

mat/0605430.

⁶ R. E. Cohen, I. I. Mazin, and D. G. Isaak, *Science* **275**, 654 (1997).

⁷ T. Kondo, T. Yagi, Y. Syono, Y. Noguchi, T. Atou, T. Kikegawa, and O. Shimomura, *J. Appl. Phys.* **87**, 4153 (2000).

⁸ C. S. Yoo, B. Maddox, J.-H. P. Klepeis, V. Iota, W. Evans, A. McMahan, M. Y. Hu, P. Chow, M. Somayazulu, D. Hausermann, R. T. Scalettar, and W. E. Pickett, *Phys. Rev. Lett.* **94**, 115502 (2005).

⁹ J. R. Patterson, C. M. Aracne, D. D. Jackson, V. Malba, S. T. Weir, P. A. Baker, and Y. K. Vohra, *Phys. Rev. B* **69**, 220101(R) (2004).

¹⁰ L. Wagner and L. Mitás, *Chem. Phys. Lett.* **370**, 412

- (2003).
- ¹¹ L. K. Wagner and L. Mitas, cond-mat/0610088.
 - ¹² S. G. Louie, S. Froyen, and M. L. Cohen, Phys. Rev. B **26**, 1738 (1982).
 - ¹³ J.-H. Cho and M. Scheffler, Phys. Rev. B **53**, 10685 (1996).
 - ¹⁴ G. Kresse and D. Joubert, Phys. Rev. B **59**, 1758 (1999).
 - ¹⁵ A. Kiejna, G. Kresse, J. Rogal, A. De Sarkar, K. Reuter, and M. Scheffler, Phys. Rev. B **73**, 035404 (2006).
 - ¹⁶ P. Blaha, K. Schwarz, G. K. H. Madsen, D. Kvasnicka, and J. Luitz, *WIEN2k, An Augmented Plane Wave + Local Orbitals Program for Calculating Crystal Properties* (Techn. Universität Wien, Austria, 2001).
 - ¹⁷ Y. Lee, private communication.
 - ¹⁸ M. Dolg, U. Wedig, H. Stoll, and H. Preuss, J. Chem. Phys. **86**, 866 (1987).
 - ¹⁹ V. Saunders, R. Dovesi, C. Roetti, R. Orlando, C. M. Zicovich-Wilson, N. M. Harrison, K. Doll, B. Civalleri, I. Bush, P. D'Arco, and M. Llunell, *CRYSTAL2003 User's Manual* (University of Torino, Torino, 2003).
 - ²⁰ J. P. Perdew, K. Burke, and M. Ernzerhof, Phys. Rev. Lett. **77**, 3865 (1996).
 - ²¹ J. P. Perdew, M. Ernzerhof, and K. Burke, J. Chem. Phys. **105**, 9982 (1996).
 - ²² J. Heyd, G. E. Scuseria, and M. Ernzerhof, J. Chem. Phys. **118**, 8207 (2003).
 - ²³ D. Porezag, M. R. Pederson, and A. Y. Liu, Phys. Rev. B **60**, 14132 (1999).
 - ²⁴ E. Engel, A. Höck, and S. Varga, Phys. Rev. B **63**, 125121 (2001).
 - ²⁵ M. Dolg, U. Wedig, H. Stoll, and H. Preuss, J. Chem. Phys. **86**, 2123 (1987).
 - ²⁶ M. W. Schmidt, K. K. Baldridge, J. A. Boatz, S. T. Elbert, M. S. Gordon, J. H. Jensen, S. Koseki, N. Matsunaga, K. A. Nguyen, S. J. Su, T. L. Windus, M. Dupuis, and J. A. Montgomery, J. Comput. Chem. **14**, 1347 (1993).
 - ²⁷ P.-O. Widmark, P. Malmqvist, and B. O. Roos, Theor. Chim. Acta **77**, 291 (1990).
 - ²⁸ R. Pou-Américo, M. Merchán, I. Nebot-Gil, P.-O. Widmark, and B. O. Roos, Theor. Chim. Acta **92**, 149 (1995).
 - ²⁹ I. Barin, *Thermochemical data of pure substances* (VCH, Weinheim, Federal Republic of Germany, 1993), 2nd ed.
 - ³⁰ S. Smoes and J. Drowart, High Temp. Sci. **17**, 31 (1984).
 - ³¹ Z. Fang, I. V. Solovyev, H. Sawada, and K. Terakura, Phys. Rev. B **59**, 762 (1999).
 - ³² V. Cocula, F. Starrost, S. C. Watson, and E. A. Carter, J. Chem. Phys. **119**, 7659 (2003).
 - ³³ S. C. Watson and E. A. Carter, Phys. Rev. B **58**, R13309 (1998).
 - ³⁴ I. G. Batyrev, J.-H. Cho, and L. Kleinman, Phys. Rev. B **63**, 172420 (2001).
 - ³⁵ G. Kresse, W. Bergermayer, and R. Podloucky, Phys. Rev. B **66**, 146401 (2002).
 - ³⁶ V. Cocula and E. A. Carter, Phys. Rev. B **69**, 052404 (2004).
 - ³⁷ G. Kresse, P. Blaha, J. L. F. Da Silva, and M. V. Ganduglia-Pirovano, Phys. Rev. B **72**, 237101 (2005).
 - ³⁸ S. Fabris, S. de Gironcoli, S. Baroni, G. Vicario, and G. Balducci, Phys. Rev. B **72**, 237102 (2005).
 - ³⁹ D. Vanderbilt, Phys. Rev. B **41**, 7892 (1990).
 - ⁴⁰ P. E. Blöchl, Phys. Rev. B **50**, 17953 (1994).
 - ⁴¹ The muffin-tin radii R_{MT} were set to $1.81 a_B$ for Mn atom and $1.6 a_B$ for oxygen (a_B stands for Bohr radius) and held constant for all volumes. This choice represents almost touching spheres for the smallest studied volume.
 - ⁴² In the B8 phases the Mn atoms occupy the Ni sites and oxygen atoms sit at the As sites.
 - ⁴³ The problem of a large (plane-wave) cut-off required by localized semi-core states can be successfully overcome within alternative frozen-core techniques such as ultrasoft pseudopotentials³⁹ or the projector augmented-wave (PAW) method.^{14,40}